PHILOSOPHICAL TRANSACTIONS OF THE ROYAL SOCIETY A MATHEMATICAL, PHYSICAL & ENGINEERING SCIENCES

Triply Periodic Level Surfaces as Models for Cubic Tricontinuous Block Copolymer Morphologies

Charla A. Lambert, Leonard H. Radzilowski and Edwin L. Thomas

Phil. Trans. R. Soc. Lond. A 1996 **354**, 2009-2023
doi: 10.1098/rsta.1996.0089

Triply periodic level surfaces as models for cubic tricontinuous block copolymer morphologies

By Charla A. Lambert, Leonard H. Radzilowski and Edwin L. Thomas

Department of Materials Science and Engineering, Massachusetts Institute of Technology, 77 Massachusetts Avenue, Cambridge, MA 02139, USA

The domains of microphase separated block copolymers develop interfacial surfaces of approximately constant mean curvature in response to thermodynamic driving forces. Of particular recent interest are the tricontinuous triply periodic morphologies and their mathematical representations. Level surfaces are represented by certain real functions which satisfy the expression $F(x, y, z) = t$, where t is a constant. In general, they are non-self-intersecting and smooth, except at special values of the parameter t. We construct periodic level surfaces according to the allowed reflections of a particular cubic space group; such triply periodic surfaces maintain the symmetries of the chosen space group and make attractive approximations to certain recently computed triply periodic surfaces of constant mean curvature. This paper is a study of the accuracy of the approximations constructed using the lowest Fourier term of the $Pm\bar{3}m$, $Fd\bar{3}m$ and $I4_132$ space groups, and the usefulness of these approximations in analysing experimentally observed tricontinuous block copolymer morphologies at a variety of volume fractions. We numerically compare surface area per unit volume of particular level surfaces with constant mean curvature surfaces having the same volume fraction. We also demonstrate the utility of level surfaces in simulating projections of tricontinuous microdomain morphologies for comparison with actual transmission electron micrographs and determination of block copolymer microstructure.

1. Introduction

Block copolymers are materials with microstructural features that exhibit a rich variety of interfacial surface curvature. Understanding of this behaviour is important not only for the prediction of material properties but also for insight into the interdependence of curvature and macromolecular physics. This creates a need for merging experimental polymer materials physics with aspects of differential geometry.

Block copolymers consist of chemically different macromolecules, or *blocks*, joined at their endpoints to form a chain. The A and B blocks desire to segregate from each other, but being restricted by their connectivity they form microdomains that are periodic on the length scale of the macromolecule (Bates & Fredrickson 1990; Thomas & Lescanec 1994). At thermodynamic equilibrium and when the segregation power is large, the A and B blocks arrange themselves so as to define an interface, the *intermaterial dividing surface* (IMDS). The shape that the IMDS prefers to adopt reflects

Phil. Trans. R. Soc. Lond. A (1996) **354**, 2009–2023
Printed in Great Britain

the need to minimize the number of energetically unfavourable contacts between unlike blocks. Since the number of contacts are proportional to area, this leads to the local minimization of the IMDS area. Such surfaces in microphase-separated block copolymers have been observed to have constant mean curvature (CMC) (Thomas *et al.* 1988). This behaviour is somewhat analogous to that of surfactant–water mixtures (see, for example, Tate *et al.* 1991; Charvolin & Sadoc 1987), except that in high molecular weight polymers an entropic penalty due to the stretching of chains away from *both* sides of the microdomain boundary is significant. Formation of a periodic morphology, however, helps to alleviate the penalty. Indeed, it is the competition between chain stretching and area minimization that determines the type of morphology at a given *volume fraction*, or ϕ. Unlike surfactant–water systems, where fluctuations on the length scale of the molecules are significant, the notion of a smooth surface separating the components in strongly segregated block copolymer systems is a quite reasonable approximation. By proper choice of copolymer, one or both of the blocks can be below its glass transition temperature so that the structure of the solid sample can be directly visualized by TEM at room temperature.

Among the periodic CMC microdomain structures that occur in A/B diblock copolymers are, with increasing volume fraction of A, lamellae of A and B, cylinders of B in a matrix of A and spheres of B in a matrix of A. Inverse morphologies occur for increasing volume fraction of B. Beyond diblocks are more complex multiblock copolymers composed of more than two different blocks (e.g. A/B/A or A/B/C) linked in a linear (triblock, tetrablock, etc.) or in a branched (e.g. star) configuration (Bi & Fetters 1975; Fetters 1969). In addition to the above three microdomain morphologies, linear multiblock copolymers have shown several unique morphologies (see, for example, Stadler *et al.* 1995). All of these microstructures, however, are examples of *unconnected* periodic arrangements of IMDS. Two connected morphologies that have been observed for simple diblocks, star diblocks and ABC triblocks are the tricontinuous double diamond (Thomas *et al.* 1986; Hasegawa *et al.* 1987; Mogi *et al.* 1992; Matsushita *et al.* 1994) and the tricontinuous double gyroid (Hajduk *et al.* 1994; Schulz *et al.* 1994). Based on the cubic space groups $Pn\bar{3}m$ and $Ia\bar{3}d$, respectively, the microstructures contain IMDSs which partition space into three continuous subvolumes comprised of two triply periodic labyrinths of the minority block embedded in a matrix of the majority block. The labyrinths have equal volume, and ϕ in each case may be expressed as $\frac{1}{2}$A/B/$\frac{1}{2}$A. Experimentally observed volume fractions for the tricontinuous cubic structures range from approximately 13 to 19% for one of the minority labyrinths. The total minority component volume fractions lie between those of cylinder and lamellar morphologies. Interestingly, we have recently observed a tricontinuous morphology in an A/B multiblock copolymer (miktoarm, or mixed-arm star) (Tselikas *et al.* 1996) having a volume fraction of 50/50 (i.e. 25/50/25).

Because cubic morphologies have been observed at a variety of volume fractions, the need has arisen to model *families* of triply periodic surfaces. Only a few triply periodic surfaces of constant mean curvature are explicitly known to exist; only five families in cubic space groups have been numerically computed (four by Anderson, one by Große-Brauckmann). The level surfaces we examine here are trigonometric functions which maintain the symmetries of one of three of these cubic space groups. Families of level surfaces are easily obtained through variation of the characteristic constant, $t = F(x, y, z)$. The advantages of studying these level surface families, or *level sets*, as approximations to CMC surfaces are two-fold: they present an immediate solution to the need for families of triply periodic models; and they provide insight

PHILOSOPHICAL TRANSACTIONS OF THE ROYAL SOCIETY A MATHEMATICAL, PHYSICAL & ENGINEERING SCIENCES

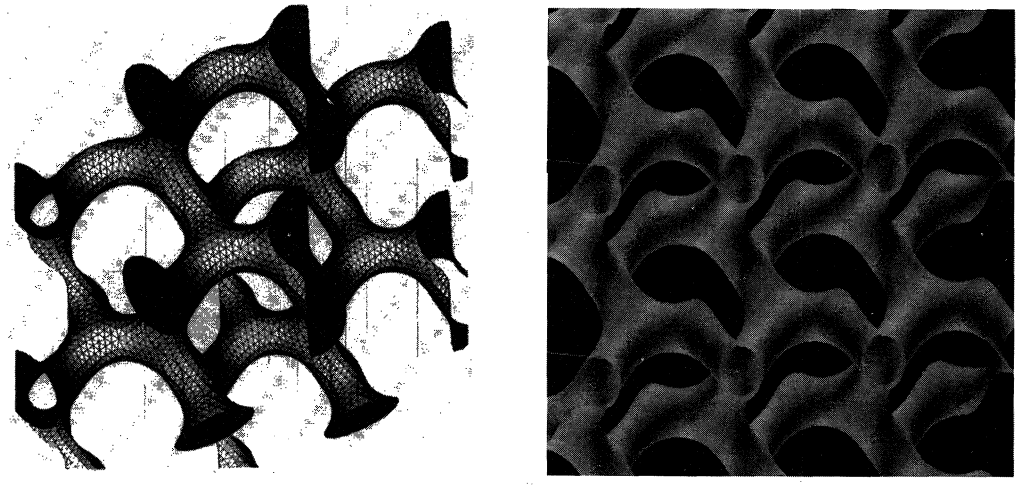

(*a*) (*b*)

Figure 1. (*a*) One labyrinth of the 18.75% minority volume fraction constant mean curvature double gyroid (courtesy of Große-Brauckmann 1995). (*b*) The level surface double gyroid model with the same minority volume fraction, $t = \pm 0.972$, as generated by TEMsim.

into how connected surfaces in those cubic space groups which do not yet have known CMC families behave as ϕ is varied, though we do not examine this aspect here. Wohlgemuth & Thomas (1996) provide an introduction for the computation of level sets and the extension of periodic level sets to other space groups.

In the present paper, we direct our attention to the P, D, and G CMC and level surface families. The accuracy of the first allowed reflection level surface approximations to CMCs varies from family to family, depending on the space group involved. We choose the P, D and G families precisely because members of D and G families have been observed as candidate intermaterial dividing surfaces in block copolymer systems. We use the software, TEMsim, written by J. T. Hoffman (Hoffman *et al.* 1994) which generates one or more models based on level surfaces of specified t values for a particular space group. Properties such as volume fraction and surface area, which we use extensively in this paper, may be measured; moreover, two-dimensional volume projections may be made of various three-dimensional model surfaces for comparison with images of block copolymers obtained by TEM. Figure 1 shows a visual comparison of the 18.75% minority volume fraction constant mean curvature double gyroid of Große-Brauckmann with the corresponding level surface approximation generated by TEMsim.

2. Approximations for constant mean curvature families

Formally, a *minimal surface* minimizes area among all nearby surfaces produced by local perturbations of the initial structure with respect to a fixed boundary. Note that the surface is globally not of absolute minimum area; in fact, minimal surfaces are often of local maximum area within their respective families (Hildebrandt & Tromba 1985). Finding a minimal surface is equivalent to solving the so-called Plateau problem: find a surface of least area spanning a given closed loop. Such solutions are physically represented by the equilibrium state of a soap film spanning a wire frame. In 1865, Schwarz published the first example of a triply periodic minimal surface, a

PHILOSOPHICAL TRANSACTIONS OF THE ROYAL SOCIETY A MATHEMATICAL, PHYSICAL & ENGINEERING SCIENCES

surface in which *mean curvature*, or H, is identically zero. The surface, now known as Schwarz's D (or diamond) surface (Schwarz 1890), was the first analytical solution to Plateau's problem that was triply periodic and embedded. Minimal surfaces were first recognized by Scriven (1976) as candidate morphologies for surfactant-water microemulsions, and later for the cubic phases of lipid–water systems (Lindblom *et al.* 1979; Longley & McIntosh 1983). Since the connection made by Scriven, a great deal of activity has ensued based on this key notion (see, for example, Sadoc 1990).

Schwarz proved the existence of four additional periodic minimal surfaces, among them the P (or primitive) surface, a surface related to the D surface through the Gauss–Bonnet transformation. Although minimal surfaces themselves have been studied intensively since the 1930s, virtually no work was done on periodic minimal surfaces until 1970, when Schoen hypothesized the existence of an additional thirteen (Schoen 1970). It was mainly through scientific interest in these surfaces as models for surfactant–water phases, zeolites and block copolymer microdomain structures that the mathematical community became aware of Schoen's pioneering work. One of the triply periodic minimal surfaces key to our research is Schoen's G surface, or *gyroid* (see figure 7 in Schoen 1970). In the 1980s, Fisher & Koch (1989) described, from a crystallographic point of view, more than thirty other candidate periodic minimal surfaces. The gyroid has only recently been rigorously proven to exist (for the method, see Karcher 1989; for the proof of embeddedness, see Große-Brauckmann & Wohlgemuth 1995); most of the rest are based solely on physical models and do not yet have existence proofs nor analytical or numerical representations (for an example computation of a minimal surface, see Cvijović & Klinowski 1994).

Minimal surfaces have everywhere vanishing mean curvature, or $H = 0$. Only within the past few years have certain triply periodic $H = \text{const.} \neq 0$ surfaces been thoroughly studied. Surfaces of constant non-zero mean curvature are characterized by the condition that they minimize area subject to a volume constraint. In 1990, Anderson *et al.* numerically discovered CMC families for the P, D, I–WP, F–RD, and S′–S″ minimal surfaces (Anderson *et al.* 1990), the first four of which are cubic (the last has tetragonal symmetry). In 1995, using Brakke's surface evolver (Brakke 1992), Große-Brauckmann computed the CMC family of the G minimal surface. Such CMC families consist of the triply periodic embedded minimal surface, along with two branches of associated surfaces (also triply periodic and embedded), one for each sign of mean curvature. Each $H = \pm\,\text{const.}$ pair of surfaces consists of two intertwined but disjoint labyrinths lying on either side of the infinitely connected minimal surface. Each labyrinth alone maintains the same symmetries as the minimal surface. The two labyrinths together can be symmetric, as in the P and D families, or not, as in the I–WP and F–RD families. The G family is somewhat special, as it consists of labyrinths which are of opposite hand.

In 1986, the first triply periodic connected microdomain morphology in block copolymers was discovered (Thomas *et al.* 1986). The members of the CMC family based on Schwarz's D surface were introduced in 1988 as candidate intermaterial dividing surfaces for such block copolymer structures (Thomas *et al.* 1988; Anderson & Thomas 1988). Subsequent research has shown that many block copolymer materials exhibit triply periodic connected microdomains possessing either $Pn\bar{3}m$ or $Ia\bar{3}d$ symmetry. To understand what molecular factors bring about the occurrence of these novel structures, a quantitative description of the microdomain geometry as a function of composition is necessary. Level surfaces can readily serve this need. Our level sets are constructed by varying the parameter t. Generally speaking, t is a

PHILOSOPHICAL TRANSACTIONS OF THE ROYAL SOCIETY A MATHEMATICAL, PHYSICAL & ENGINEERING SCIENCES

constant representing the offset of a level surface from the $t = 0$ base surface. Note that the offset is not a distance; if it were, we would instead be discussing families of *constant thickness* surfaces, which are introduced briefly later. The parameter t is instead related to a monotonic decrease (or increase) in volume fraction. To model the tricontinuous block copolymer systems with level sets resulting in the desired $\frac{1}{2}$A/B/$\frac{1}{2}$A volume fraction, the function $F(x, y, z)$ is set equal to $\pm$const.. Because the triply periodic surfaces we construct have inversion symmetry, the $t = 0$ surface in each family divides space into two equal subvolumes. Thus, our trigonometric level sets consist of the $t = 0$ surface along with two branches of symmetry-preserving surfaces, one for each sign of t. Structures where the two A components are not equal can also be modelled with level surface families by choosing constants for t which are not equal in magnitude; this procedure can be carried out for any number of tricontinuous labyrinths.

To construct a level surface with a particular space group symmetry, one uses the *International tables for X-ray crystallography* to find the set of allowed $\{hkl\}$ values of the Fourier components of the structure and the Fourier series representation of the space group. The general expression for the density distribution within the unit cell for the particular space group can then be computed using the lowest order allowed value of $\{hkl\}$. Every allowed component results in one surface with the desired symmetry, and linear combinations of the components result in even more; the lowest-order Fourier term seems to give the simplest surface. Wohlgemuth & Thomas (1996), who developed this procedure, obtained equations for the P, D and G level surface families (given in the next section) using the first Fourier component only.

A second procedure for generating trigonometric functions, the zero sets of which are periodic surfaces with a desired symmetry, is the *nodal surfaces* technique. Von Schnering & Nesper (1987) demonstrated the close resemblance between certain truncated Fourier series that represent equipotential surfaces and certain triply periodic minimal surfaces. In fact, the truncated equipotential series expressions obtained by Barnes (1990) for P, D and G are the same as those obtained for the respective level surfaces by Wohlgemuth & Thomas (1996) though by a different procedure. Nodal surfaces have only been analysed when their function values are zero.

Another approach to generating candidate model surfaces for microstructural research involves the use of minimal surfaces as base surfaces for the construction of *parallel*, or *constant thickness surfaces*, which are used in modelling periodic IMDSs. Given a base reference surface in space, we can define a parallel surface by moving a fixed distance along the local normals. Pairs of such surfaces constructed from base minimal surfaces have been found to approximate well some members of the triply periodic CMC families (Anderson *et al.* 1988). The local mean curvature of a parallel surface is easily calculated from the principal curvatures of the base surface; however, curvature singularities develop when the distance moved along the normals is approximately the size of either principal radius. The recent discovery of the double gyroid morphology in diblock copolymers by Hajduk *et al.* (1994) proposed a member of the family of parallel surfaces based on Schoen's gyroid as an appropriate model for the equilibrium morphology. Whether the precise IMDS of the phase separated block copolymer is closer to a parallel surface, CMC surface, or some other surface is, at present, an open question.

3. Behaviour of level surfaces

Consider level surfaces of triply periodic functions with cubic symmetry $F(x, y, z) = t$. In our examples, the parameter which distinguishes members of a

given family of level surfaces is t. For a positive value of t, a surface results which is to one side of the $t = 0$ surface; a negative value results in a surface at the same offset on the other side. Since our examples include a point of inversion on $F(x, y, z) = 0$, $\pm t$ results in a symmetrical pair of surfaces. Thus, the $t = 0$ surface divides space equally, and pairs of level surfaces, $\pm t$, divide space into three tricontinuous subvolumes with volume fractions $\frac{1}{2}$A/B/$\frac{1}{2}$A. The trigonometric functions for the P (space group $Pm\bar{3}m$, {100} Fourier component), D (space group $Fd\bar{3}m$, {111} Fourier component) and G (space group $I4_132$, {110} Fourier component) level surface families are given by the following three equations, respectively:

$$\cos x + \cos y + \cos z = t, \quad (3.1)$$

$$\sin x \sin y \sin z + \sin x \cos y \cos z + \cos x \sin y \cos z + \cos x \cos y \sin z = t, \quad (3.2)$$

$$\sin x \cos y + \sin y \cos z + \sin z \cos x = t. \quad (3.3)$$

As t is increased in magnitude, the family members pull away from the $t = 0$ surface in the same fashion that CMC and parallel surfaces pull away from minimal surfaces. Triply periodic cubic-symmetry level surfaces decrease monotonically in both surface area and labyrinth volume with increase in the absolute value of t; they terminate by 'pinching off', or becoming disconnected, and eventually disappear altogether. Figure 2 shows the variation of ϕ with t for each of the three families considered. Note that the graph for the P family in particular is approximately linear up to $t = 1$, and then drops off faster. In general, this is true for all three families: ϕ decreases linearly with t until the surfaces 'pinch-off', then it drops off faster and eventually disappears. In the D and G families, the point at which the surfaces become disconnected is so near the maximum t value that the graphs appear completely linear. It is straightforward to see how and why the families terminate by disappearing. The maximum magnitude that t can reach in the P family, for example, is 3; therefore, the P family disappears at $t = \pm 3$. By the same reasoning, the D family disappears at $t = \pm\sqrt{2}$ and the G family disappears at $t = \pm 1.5$.

With triply periodic CMC surfaces of cubic symmetry, the parameter which effectively distinguishes different surfaces in a family is mean curvature, or H. As H increases in magnitude, the interpenetrating networks gradually pull farther away from the minimal surface, decreasing in both area and volume, until a single H value is reached for which both the minimum surface area and minimum labyrinth volume of the entire family is reached. After this point, the behaviour of volume fraction in these CMC families becomes more complicated, as indicated in figure 3, which shows the variation of H over a range of volume fractions (Anderson *et al.* 1990). The maximum mean curvatures for the P and D families are marked on the graphs as 2.133 and 5.6, respectively (the maximum mean curvature in the G family is 5.52, from Große-Brauckmann (1995)). The family members with these values for H become disconnected. Past this point, all CMC surfaces are disconnected, mean curvature decreases and the families finally terminate in close-packed spheres of the appropriate symmetry.

4. Relationships between level surfaces and surfaces of constant mean curvature

Because level surfaces have neither constant mean curvature nor an area that can predictably relate to those of CMC surfaces, volume fraction was the characteristic used to relate our level surface families to the P, D and G CMC families. Table 1

PHILOSOPHICAL TRANSACTIONS OF THE ROYAL SOCIETY A MATHEMATICAL, PHYSICAL & ENGINEERING SCIENCES

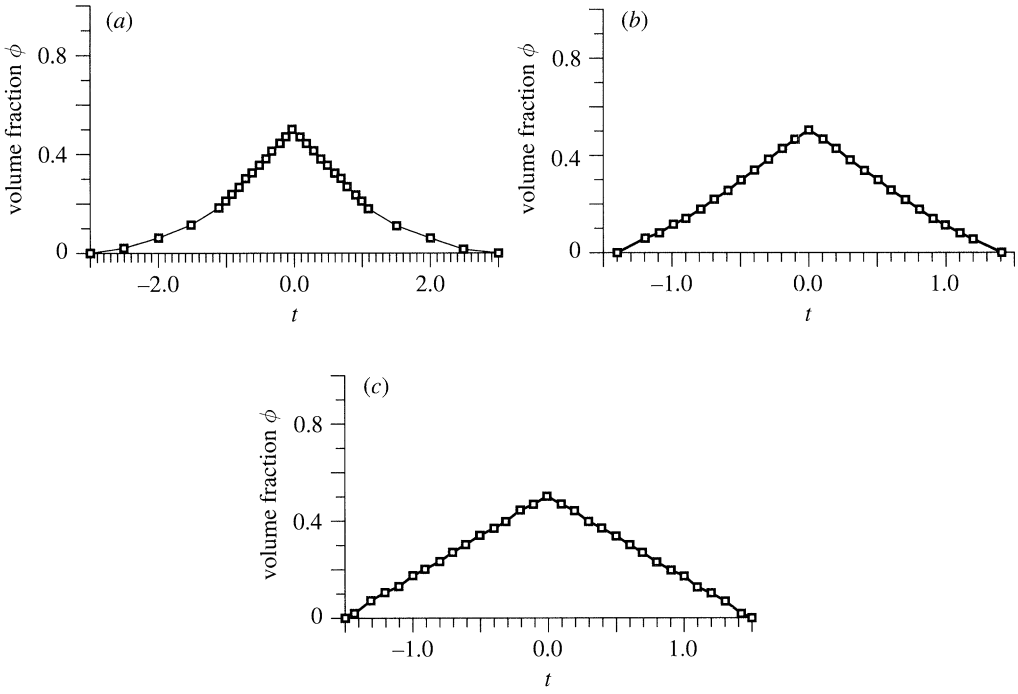

Figure 2. The behaviour of volume fraction in the (*a*) P, (*b*) D and (*c*) G level surfaces families. The figures give volume fraction as a function of t.

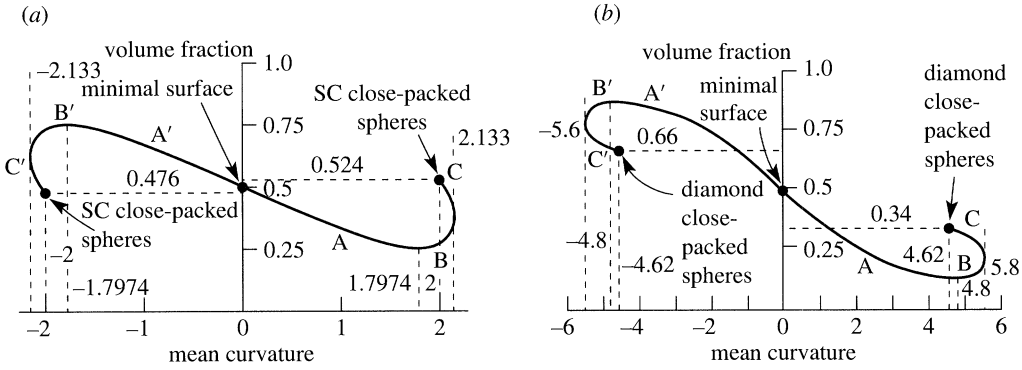

Figure 3. The behaviour of volume fraction for surfaces of constant mean curvature: (*a*) P family; (*b*) D family. The figures, taken from Anderson (1990) on periodic surfaces of prescribed mean curvature, give volume fraction as a function of H; the G family exhibits similar behaviour, as documented in Große-Brauckmann (1995).

lists the particular surfaces used in our comparisons. The 25/50/25 pairs of surfaces in each family, along with the 'experimentally observed' double-diamond and double-gyroid surfaces, were studied specifically because of their direct applications to block copolymer and water–surfactant systems; the other four distinguished surfaces were chosen for completeness. All values for H and ϕ for the constant mean curvature surfaces were taken from Anderson *et al.* (1990) and Große-Brauckmann (1995). The minimal, minimum-area and volume, and pinch-off surfaces themselves are highlighted and discussed in detail in both of these papers. The corresponding level surface function values, t, were calculated by assuming the approximately linear

Table 1. *Distinguished level surfaces and surfaces of constant mean curvature*

(Volume fractions given in all our tables are those of the minority phase A, for the bicontinuous minimal surfaces and their approximations, or $\frac{1}{2}$A, for the tricontinuous surfaces. The 'experimentally observed' surfaces in the D and G families are discussed in Anderson & Thomas (1988) and Hajduk *et al.* (1994), respectively.)

	P family			D family			G family		
description	H	ϕ	t	H	ϕ	t	H	ϕ	t
minimal surface	0	0.5	0.0	0	0.5	0.0	0	0.5	0.0
25/50/25 surface	1.755	0.25	0.862	2.1	0.25	0.694	1.317	0.25	0.778
experimentally observed				4.78	0.131	1.025	1.848	0.1875	0.972
minimum area and volume family member	1.7974	0.2487	0.866	4.8	0.130 85	1.0254	5.29	0.056	1.38
pinch-off CMC surface	2.133	0.353 99		5.6	0.18		5.52	0.069	
pinch-off level surface		0.210 29	0.999		0.140 72	0.998		0.046	1.413

behaviour between volume fraction and function parameter illustrated in figure 2. A comparison of experimental values, those taken directly from TEMsim, and calculated values, those taken from the graphs of figure 2, is provided in table 2.

The last row in table 1 gives the ϕ and t values for the pinch-off surface in each family; the next row up gives the H and ϕ values for the corresponding surface of constant mean curvature. Note that the volume fractions for these two pinch-off surfaces differ by more than 14% in the P family, but are within 2–4% of each other in both the D and G families. This is a direct result of the nonlinear behaviour that the CMC volume fractions exhibit. However, cubic tricontinuous structures are candidate morphologies in PS–PI block copolymer systems only at minority volume fractions $\frac{1}{2}$A of approximately 13–25%. This range is well within the values for t which are consistent with the corresponding CMC volume fractions. The only exception to this is the experimentally observed double diamond; though the CMC surface is connected at 13.1% minority volume fraction, its corresponding level surface, $t = \pm 1.025$, is disconnected.

The relationships between surface area per unit volume and t for the P, D and G level surface families are approximately described by concave parabolas centred around $t = 0$. Figure 4*a* shows the variation of surface area per unit volume with volume fraction for each of the level surface families; the behaviour is also approximately parabolic with a maximum at $\phi = 50\%$. The values for surface area were calculated over the range of volume fraction using TEMsim for a standard unit cell of volume π^3. The volume fractions at which the surfaces pinch-off are indicated by arrows. For this particular normalization, the P level surface family has the least surface area over all values of ϕ; the D family has the largest area until a crossover occurs with the G family around $\phi = 11\%$. Least area is a consideration for candidate models of block copolymer IMDSs because of the need to minimize the number

Table 2. *Comparisons of experimental and calculated values for t*

(The experimental values were determined directly from the TEMsim volume fraction statistic; they are the data points for the level surface graphs in figure 2. The calculated values are those found by assuming a linear relationship between level surface volume fractions and t; they are the function values corresponding to the data points in figure 2.)

description	ϕ	experimental	calculated
P family			
25/50/25 surface	0.25	0.9	0.862
minimum area and volume family member	0.248 77	0.9	0.866
D family			
25/50/25 surface	0.25	0.6	0.694
experimentally observed	0.131	1.03	1.025
minimum area and volume family member	0.130 85	1.03	1.0254
G family			
25/50/25 surface	0.25	0.762	0.778
experimentally observed	0.1875	0.948	0.972
minimum area and volume family member	0.056	1.32	1.38

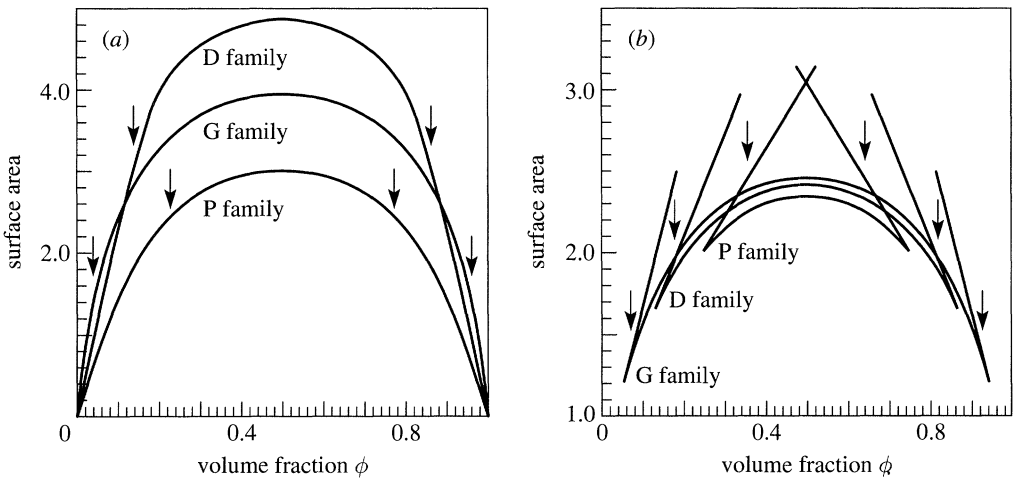

Figure 4. The variation of surface area with volume fraction: (*a*) surface area per unit volume against ϕ for the P, D and G level surface families; (*b*) surface area per unit volume of the the translational fundamental domain as plotted against ϕ in each of the corresponding CMC families. Volume fractions at which pinch-off of surfaces occurs are indicated by arrows.

of energetically unfavourable contacts between unlike blocks. Thus the model with least IMDS area may prove to be energetically more favourable.

Figure 4*b* reproduces the relationship between surface area per unit volume and volume fraction for the corresponding P, D and G CMC families. The data was extrapolated from Anderson *et al.* (1990) and Große-Brauckmann (1995) and normalized

using Große-Brauckmann's technique based on the translational fundamental domain in each minimal surface. For $25\% \leqslant \phi \leqslant 50\%$, the P CMC family has the least surface area; for $13\% \leqslant \phi \leqslant 25\%$, the D family is lowest in area, and the G family is then lowest until $\phi = 5.6\%$, where the minimum area and volume surface occurs in the family. Note that the behaviour of our triply periodic level sets is similar to that of the corresponding CMC families around $\phi = 50\%$.

Various possible normalization schemes exist for comparison between families of surfaces. For example, Große-Brauckmann considers, among others, normalizing the volume of the respective translational fundamental cell to unity. For our level sets, we choose to normalize the standard cell across all three families to unity. The relative rankings of the P, D and G surface areas (with respect to volume fraction) changes depending on the choice of normalization; the proper normalization depends on the problem under consideration. In dealing with block copolymers, molecular weight is a constraint in addition to volume fraction. These two parameters together set the preferred length scales of the domains defined by an IMDS.

5. Calculating mean curvatures

In addition to determining the behaviour of level surface families with respect to area and volume fraction, we also wished to analyse the distribution of curvature over the surfaces. This, too, was accomplished using TEMsim, which creates a surface for a given value of t using Solsurf, another program developed principally by J. T. Hoffman. Solsurf computes piecewise approximations of zero-sets of functions in three variables (Hoffman & Hoffman 1994, personal communication). It implicitly solves the appropriate level surface equation (as given by (3.1)–(3.3)) for a list of x, y and z values, with the constraint that only a few points are needed in places of low curvature, and many points are needed in places of high curvature. To compute the distribution of curvatures on the P, D and G level surfaces, we extracted these lists of points (within five-digit accuracy of the particular t value) and calculated the local mean (H) curvatures used the following second-order differential equation:

$$H = \frac{f_x^2(f_{yy}+f_{zz}) + f_y^2(f_{xx}+f_{zz}) + f_z^2(f_{xx}+f_{yy}) - 2(f_x f_y f_{xy} + f_y f_z f_{yz} + f_x f_z f_{xz})}{2(f_x^2+f_y^2+f_z^2)^{3/2}}. \tag{5.1}$$

Figure 5 gives the results of the mean curvature calculations for the minimal surface approximations ($t = 0$) in each level surface family. It is intuitive that the mean curvature values should be evenly distributed around $H = 0$; the surfaces are approximations to those with everywhere vanishing mean curvature. In fact, due to the inversion symmetry of each of the space groups, the distribution of H must be symmetric about zero for *all* surfaces in each of the level surface families, though, for example, one might expect even distributions around 4.78 and 1.848 for the 13.1% double-diamond and 18.75% double-gyroid approximations, respectively. This is in contrast to CMC families, in which H varies in a complex manner with volume fraction (see figure 3).

6. Experimental and simulated volume projections

Most experimental data on block copolymer morphology come from the complimentary methods of transmission electron microscopy (TEM) and small-angle X-ray

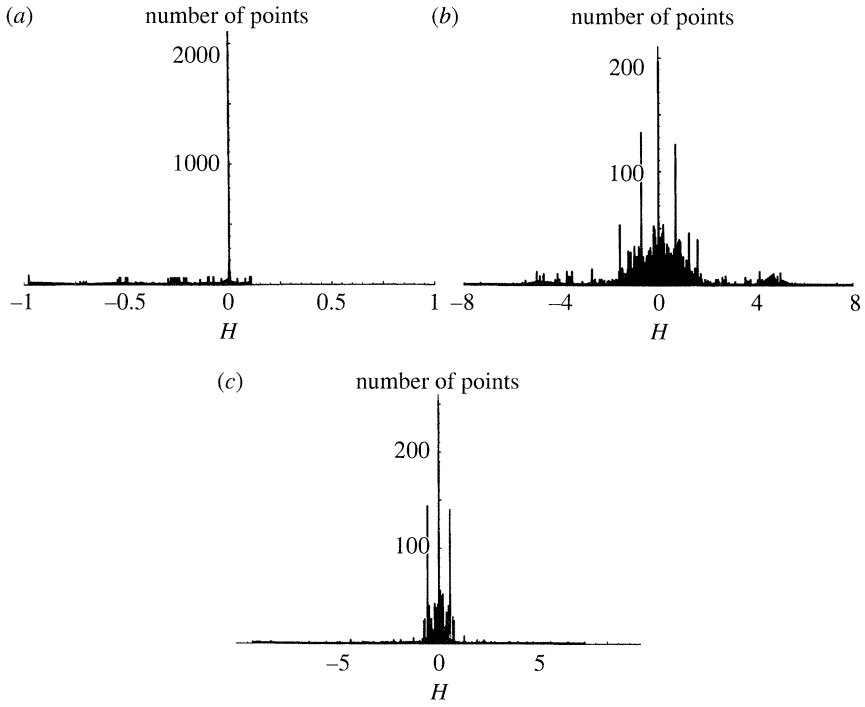

Figure 5. Mean curvature values for $t = 0$ surfaces: (*a*) P surface; (*b*) D surface; (*c*) G surface. Note that the distribution of the P surface, though not symmetrical around $H = 0$, has substantially more points at $H = 0$ than either the D or G surfaces. Thus, the average mean curvature across each of the surfaces is approximately the same, and close to zero.

scattering (SAXS). In TEM, the observed image is a two-dimensional projection of a three-dimensional object, interpretation of which is inherently ambiguous. Depending on the complexity of the object, more information may be obtained by gathering projections with the sample tilted to different orientations in the TEM. Indeed, a three-dimensional reconstruction of the object may be performed using a series of projections taken at incremental angles of sample tilt (see, for example, Frank 1992). An alternative approach is through the use of computer algorithms that simulate projections of competing model structures. Particularly appealing for microphase separated block copolymers are algorithms that utilize dividing surfaces that separate volumes of different atomic potential (Anderson *et al.* 1992). The projection capability of TEMsim is based on such an algorithm, and in this section we describe and compare it with TEM image formation.

In a TEM an electron beam passes through, and at the same time interacts with, a sufficiently thin (typically less than 100 nm) specimen. The interactions of the incident electrons with the specimen and the operation of the microscope combine to produce the observed image. Specimens of block copolymers with approximately equilibrium microdomain structures typically 20–50 nm in size are produced by solvent casting of films followed by long-term annealing. Thin (*ca.* 50 nm) sections are then cut from films using an ultramicrotome.

Sections may then be preferentially stained with a compound containing a heavy atom such as osmium tetroxide. The vapors of this compound selectively react with the carbon–carbon double bonds of polydienes, depositing osmium atoms in diene-rich domains. In the TEM, incident electrons interact with the stained specimen to

produce amplitude–mass thickness contrast. The transmitted bright field image intensity I_t at a point (x, y) in the final image plane may be approximately given by

$$I_t(x, y) = I_0 - I_0 \int_{-h/2}^{h/2} \rho(x, y, z)\, \mathrm{d}z, \tag{6.1}$$

where I_0 is the intensity of the incident electron beam taken parallel to the z-axis, and $\rho(x, y, z)$ is the material density at a point (x, y, z) in the sample of thickness h. Microphase separated regions containing the heavy atom stain will have a relatively larger density and hence a reduced $I_t(x, y)$ relative to unstained regions.

TEMsim uses projection parameters common to TEM which enhance its analytical capabilities. A dividing surface (or nested surfaces, in the case of a tricontinuous IMDS) is first generated in terms of the particular surface family and offset parameter and then graphically displayed in three dimensions (see, for example, figure 1*b*). The dividing surface may be viewed from any orientation specified in terms of Miller indices, (hkl) (in the cubic system the $[hkl]$ direction is normal to the (hkl) plane). It can then be 'sliced' to a specified fraction or multiple of the unit cell dimension between parallel planes, mimicking the sample preparation technique. The position within the unit cell and the orientation of the slicing planes may also be specified. A ray-tracing algorithm makes projections of the dividing surface and progressively refines the resolution. A ray is traced parallel to the viewing direction, taken as the z-axis, and is divided into segments corresponding to A and B regions at every dividing surface encountered. The relative intensity projected at a particular pixel, $I_{\mathrm{rel}}(x, y)$, is then equal to the ratio of the total lengths traced through A and B regions, and is given by

$$I_{\mathrm{rel}}(x, y) = \frac{\sum \mathrm{length_A}}{\sum \mathrm{length_A} + \sum \mathrm{length_B}}. \tag{6.2}$$

By making A the 'denser' medium (i.e. $\rho_A = 1$ and $\rho_B = 0$), equation (6.2) gives a relative intensity of one for black and zero for white.

Figure 6*a* shows a TEM micrograph of a poly(styrene)–poly(isoprene) miktoarm (mixed arm star) block copolymer (Tselikas *et al.* 1996) that has been annealed, microtomed and stained. It reveals a variety of ordered morphologies that coexist in adjacent regions, or grains, of the material and have plane groups that are (from left to right) $p2mm$, $p4mm$, and $p6mm$ (projection over a period takes $3m$ to $6mm$). The simultaneous presence of both three- and four-fold axes implies cubic symmetry, which is supported by the sample's isotropic optical properties. SAXS intensity profiles of this material are also consistent with cubic symmetry, although they lack sufficient resolution to determine a unique fit to one of the 35 cubic space groups. Because the double-diamond ($Pn\bar{3}m$) and the double-gyroid ($Ia\bar{3}d$) tricontinuous morphologies are known structures for block copolymers, TEMsim projections were conducted for these two possibilities. Projections were generated for different unit cell orientations, sample thicknesses and slice locations within the unit cell for the D and G level surface families for the appropriate sample volume fraction.

The first peak of the SAXS data occurs at 54.5 nm and corresponds to a lattice parameter of either 77.1 nm for the double-diamond or 133.5 nm for the double-gyroid structure. The section thickness is approximately in the 70–100 nm range. Thus the simulated projections were performed for slice thicknesses in the range of one to $\sqrt{3}$ times the lattice parameter. Figures 6*b–d* shows such image simulations for a tricontinuous triply periodic structure with $Pn\bar{3}m$ symmetry consisting of a pair of poly(styrene) networks in a poly(isoprene) matrix at 25/50/25 volume fraction

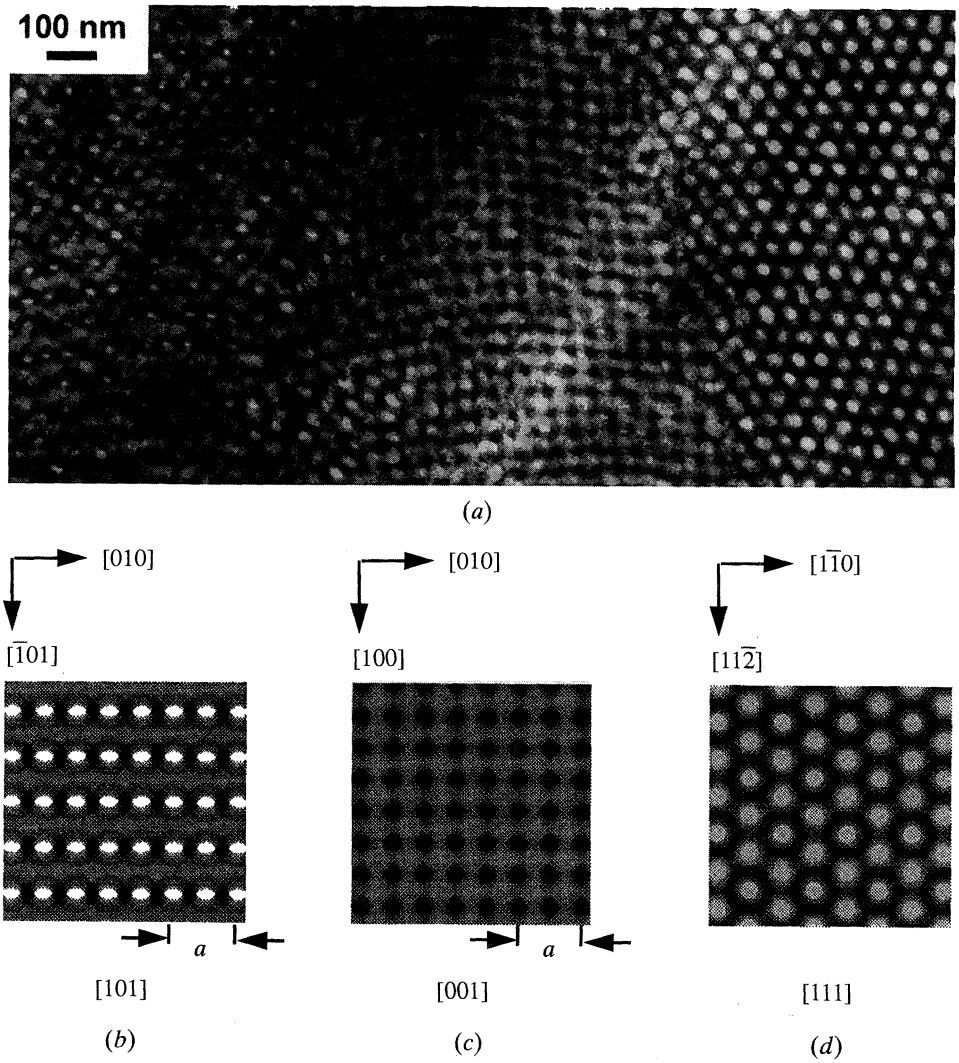

Figure 6. (*a*) Transmission electron micrograph of a microphase separated block copolymer. Three different two-dimensionally ordered patterns are apparent, each separated from the others by distinct grain boundaries. The symmetries present in these two-dimensional patterns suggest a tricontinuous morphology with cubic symmetry. Using TEMsim, projections (*b*)–(*d*) were simulated from nested D (diamond) surfaces with $t = \pm 0.694$, having volume fractions of approximately 25/50/25. (*b*) The [110] projection, (*c*) the [100] and (*d*) the [111], all of unit cell thickness, which show good agreement with the micrograph. The estimated sample thickness of that shown in (*a*) is in the range of the 77.1 nm cubic unit cell dimension for double diamond.

and one unit cell thickness. The correspondence between each region of the TEM micrograph and the respective simulation is quite good. Moreover, as the simulations do not show significant differences as a function of thickness in this range, the choice of the double-diamond microstructure is reinforced.

Also of interest are the boundaries between adjacent grains in figure 6*a*. As the axes in the figure indicate, the boundary between the left and centre grains is a 45° twist grain boundary. The boundary between the centre and right grains has both twist and tilt components. It was earlier observed that certain boundaries between

adjacent lamellar grains of A/B diblock copolymers maintained phase continuity of the respective domains across the boundary (Kinning *et al.* 1987). The nature of a lamellar boundary depends on the angle between grains: for a $\frac{1}{2}\pi$ reorientation of lamellar normals across the boundary, the structure can be represented by a minimal surface, namely 'Scherk's first surface' (Gido *et al.* 1993). Grain boundaries within tricontinuous cubic morphologies are an unexplored topic.

7. Conclusion

Families of triply periodic level surfaces with cubic symmetry have been constructed as candidates to model microdomain morphologies in block copolymers. The trigonometric formulae for the level surfaces are produced using the symmetry information for a particular space group in the *International tables for X-ray crystallography* and the lowest order Fourier component for each space group. The P, D and G level surface families are investigated and shown to be fair approximations to the respective CMC family surfaces. Mean curvature across each surface in the three level sets is evenly distributed around $H = 0$, and surface area per unit volume varies approximately like a concave parabola with volume fraction, much like the relationship observed in the corresponding CMC families. Application of level surface models to the determination of block copolymer morphology is illustrated utilizing a program, TEMsim, which produces two-dimensional projections from three-dimensional models for comparison with experimental TEM micrographs.

We thank Karsten Große-Brauckmann for providing his preprinted paper and for helpful discussions on CMC gyroids. We also thank David Hoffman and Jim Hoffman for development and support of TEMsim under grant DE-FG03-95 ER25250, and Meinhard Wohlgemuth and David Hoffman for many enlightening conversations about surfaces. Financial support was received from NSF DMR92-14853, NSF DMR94-00334(CMSE-MIT) and AFOSR F49620-94-1-0224.

References

Anderson, D. M. & Thomas, E. L. 1988 Microdomain morphology of star copolymers in the strong-segregation limit. *Macromolecules* **21**, 3221–3230.

Anderson, D. M., Davis, H. T., Scriven, L. E. & Nitsche, J. C. C. 1990 Periodic surfaces of prescribed mean curvature. *Adv. Chem. Phys.* **77**, 337–396.

Anderson, D. M., Gruner, S. M., & Leibler, S. 1988 Geometrical aspects of the frustration in the cubic phases of lyotropic liquid crystals. *Proc. Natn Acad. Sci. U.S.A.* **85**, 5364–5368.

Anderson, D. M., Bellare, J., Hoffman, J. T., Hoffman, D., Gunther, J. & Thomas, E. L. 1992 Algorithms for the computer simulation of two-dimensional projections from structures determined by dividing surfaces. *J. Coll. Interface Sci.* **148**, 398–414.

Barnes, I. 1990 A useful trigonometric approximation to periodic minimal surfaces. *Austr. Math. Soc. Gazette* **17**, 99–105.

Bates, F. S. & Fredrickson, G. H. 1990 Block copolymer thermodynamics: theory and experiment. *A. Rev. Phys. Chem.* **41**, 525–557.

Bi, L.-K. & Fetters, L. J. 1975 Domain morphology of star block copolymers of polystyrene and polyisoprene. *Macromolecules* **8**, 90–92.

Brakke, K. 1992 The surface evolver. *J. Exp. Math.* **2**, 141–165.

Charvolin, J. & Sadoc, J. F. 1987 Periodic systems of frustrated fluid films and bicontinuous cubic structures in liquid crystals. J. Physique **48**, 1559–1569.

Cvijović, D. & Klinowski, J. 1994 The computation of the triply periodic I-WP minimal surface. *Chem. Phys. Lett.* **226**, 93–99.

Fetters, L. J. 1969 Synthesis of block polymers by homogeneous anionic polymerization. *J. Polym. Sci.* C **26**, 1–35.

Fischer, W. & Koch, E. 1989 Genera of minimal balance surfaces. *Acta Crystallogr.* A **45**, 726–732.

Frank, J. (ed.) 1992 *Electron tomography: three-dimensional imaging with the transmission electron microscope.* New York: Plenum.

Gido, S. P, Gunther, J., Thomas, E. L. & Hoffman, D. 1993 Lamellar diblock copolymer grain boundary morphology. 1. Twist boundary characterization. *Macromolecules* **26**, 4506–4520.

Große-Brauckmann, K. 1995 The family of constant mean curvature gyroids. Preprint Series IV. 13, Center for Geometry, Analysis, Numerics and Graphics (GANG), University of Massachusetts, Amherst.

Große-Brauckmann, K. & Wohlgemuth, M. 1995 The gyroid is embedded and has constant mean curvature companions. Preprint SFB 256, Universität Bonn.

Hajduk, D. A., Harper, P. E., Gruner, S. M., Honeker, C. C., Kim, G., Thomas, E. L. & Fetters, L. J. 1994 The gyroid: a new equilibrium morphology in weakly segregated diblock copolymers. *Macromolecules* **27**, 4063–4075.

Hasegawa, H., Tanaka, H., Yamasaki, K. & Hashimoto, T. 1987 *Macromolecules* **20**, 1651–1662.

Hildebrandt, S. & Tromba, A. 1985 *Mathematics and optimal form.* New York: Scientific American.

Karcher, H. 1989 The triply periodic minimal surfaces of Alan Schoen and their constant mean curvature companions. *Manuscr. Math.* **64**, 291–357.

Kinning, D. J., Thomas, E. L. & Ottino, J. M. 1987 Effect of morphology on the transport of gases in block copolymers. *Macromolecules* **20**, 1129–1133.

Lindblom, G., Larsson, K., Johansson, L., Fontell, K. & Forsen, S. 1979 The cubic phase of monoglyceride-water systems. *J. Am. Chem. Soc.* **101**, 5465–5470.

Longley, W. & McIntosh, J. 1983 A bicontinuous tetrahedral structure in a liquid-crystalline lipid. *Nature* **303**, 612–614.

Matsushita, Y., Tamura, M. & Noda, I. 1994 Tricontinuous double-diamond structure formed by a styrene-isoprene-2-vinylpyridene triblock copolymer. *Macromolecules* **27**, 3680–3682.

Mogi, Y., Mori, K., Matsushita, Y. & Noda, I. 1992 Tricontinuous morphology of triblock copolymers of the ABC type. *Macromolecules* **25**, 5412–5415.

Sadoc, J. F. 1990 Geometry in Condensed Matter Physics. In *Directions in condensed matter physics*, vol. 9. Singapore: World Scientific.

Schoen, A. H. 1970 Infinite periodic minimal surfaces without self-intersections. NASA Technical Note, TN D-5541.

Schulz, M. F., Bates, F. S. & Almdal, K. 1994 Epitaxial relationship for hexagonal-to-cubic phase transition in a block copolymer mixture. *Phys. Rev. Lett.* **73**, 86–89.

Schwarz, H. A. 1890 *Gesammelte mathematische Abhandlungen.* Berlin: Springer.

Scriven, L. E. 1976 Equilibrium bicontinuous structure. *Nature* **263**, 123–125.

Stadler, R., Auschra, C., Beckmann, J., Krappe, U., Voigt-Martin, I. & Leibler, L. 1995 Morphology and thermodynamics of symmetric poly(A-*block*-B-*block*-C) triblock copolymers. *Macromolecules* **28**, 3080–3097.

Tate, M. W., Eikenberry, E. F., Turner, D. C., Shyamsunder, E. & Gruner, S. M. 1991 Nonbilayer phases of membrane lipids. *Chem. Phys. Lipids* **57**, 147–164.

Thomas, E. L., Alward, D. B., Kinning, D. J., Martin, D. C., Handlin Jr, D. L. & Fetters, L. J. 1986 Ordered bicontinuous double-diamond structure of star block copolymers: a new equilibrium morphology. *Macromolecules* **19**, 2197–2202.

Thomas, E. L., Anderson, D. M., Henkee, C. S. & Hoffman, D. 1988 Periodic area-minimizing surfaces in block copolymers. *Nature* **334**, 598–601.

Thomas, E. L. & Lescanec, R. L. 1994 Phase morphology in block copolymer systems. *Phil. Trans. R. Soc. Lond.* A **348**, 149–166.

Tselikas, Y., Hadjichristidis, N., Lescanec, R. L., Honeker, C. C., Wohlgemuth, M. & Thomas, E. L. 1995 Architecturally induced tricontinuous cubic morphology in compositionally symmetric miktoarm star block copolymers. *Macromolecules* **29**, 3390–3396.

Von Schnering, H. G. & Nesper, R. 1987 How nature adapts chemical structures to curved surfaces. *Angew. Chem. Int. Ed. Engl.* **26**, 1059–1080.

Wohlgemuth, M. & Thomas, E. L. 1996 Morphologies by symmetries. (In preparation.)

PHILOSOPHICAL TRANSACTIONS OF THE ROYAL SOCIETY A MATHEMATICAL, PHYSICAL & ENGINEERING SCIENCES

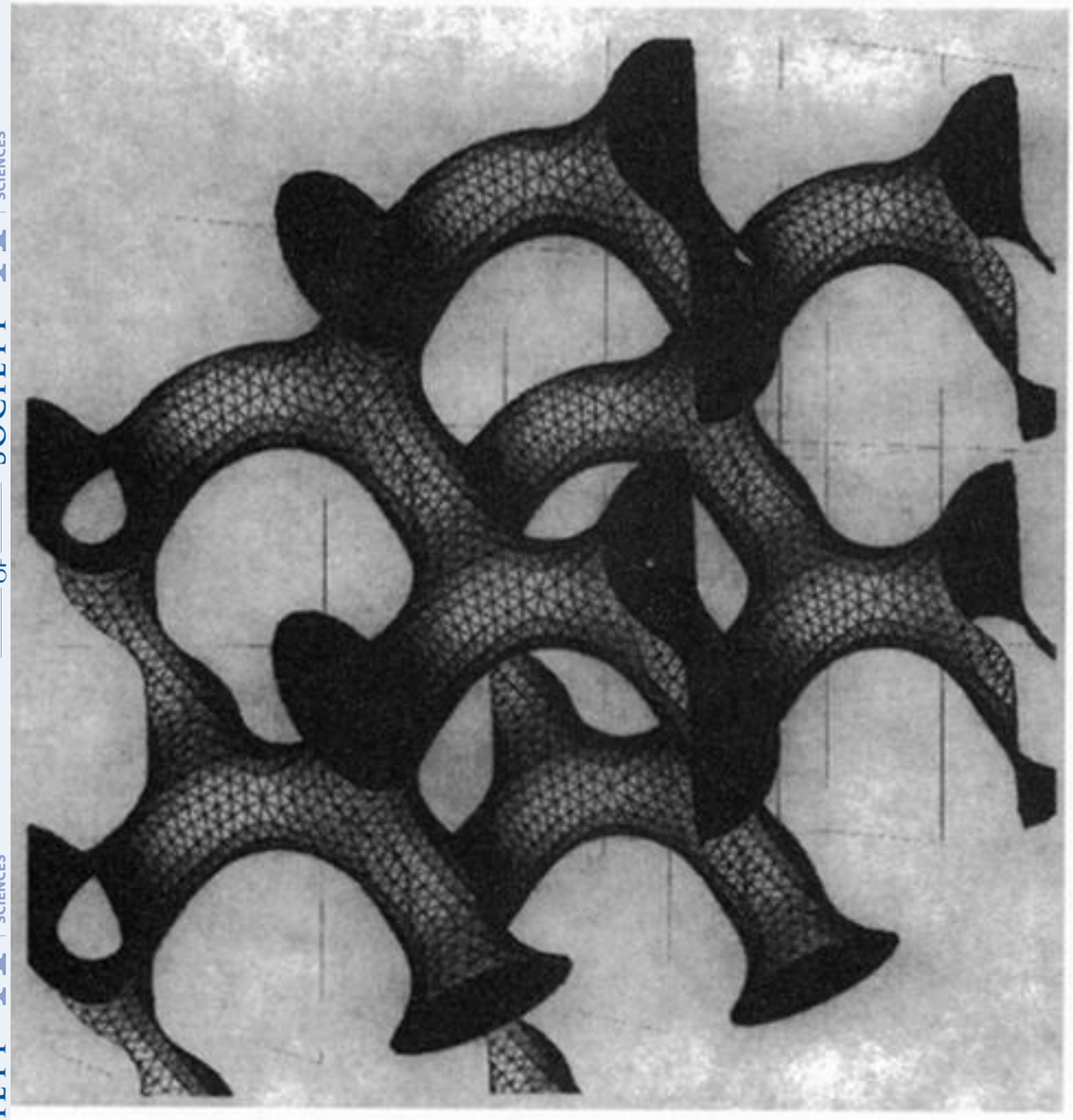

(*a*)

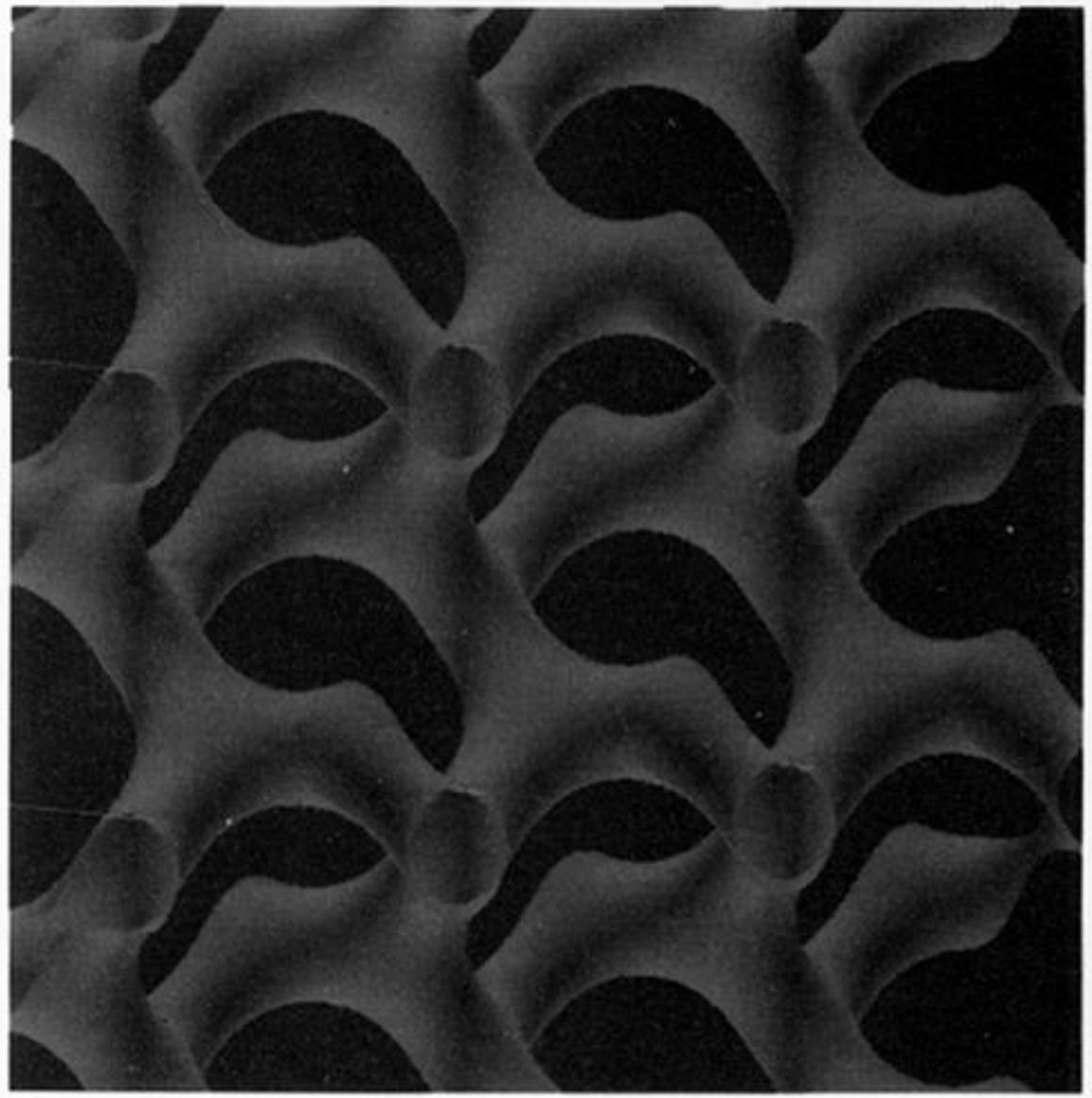

(*b*)

Figure 1. (*a*) One labyrinth of the 18.75% minority volume fraction constant mean curvature double gyroid (courtesy of Große-Brauckmann 1995). (*b*) The level surface double gyroid model with the same minority volume fraction, $t = \pm 0.972$, as generated by TEMsim.

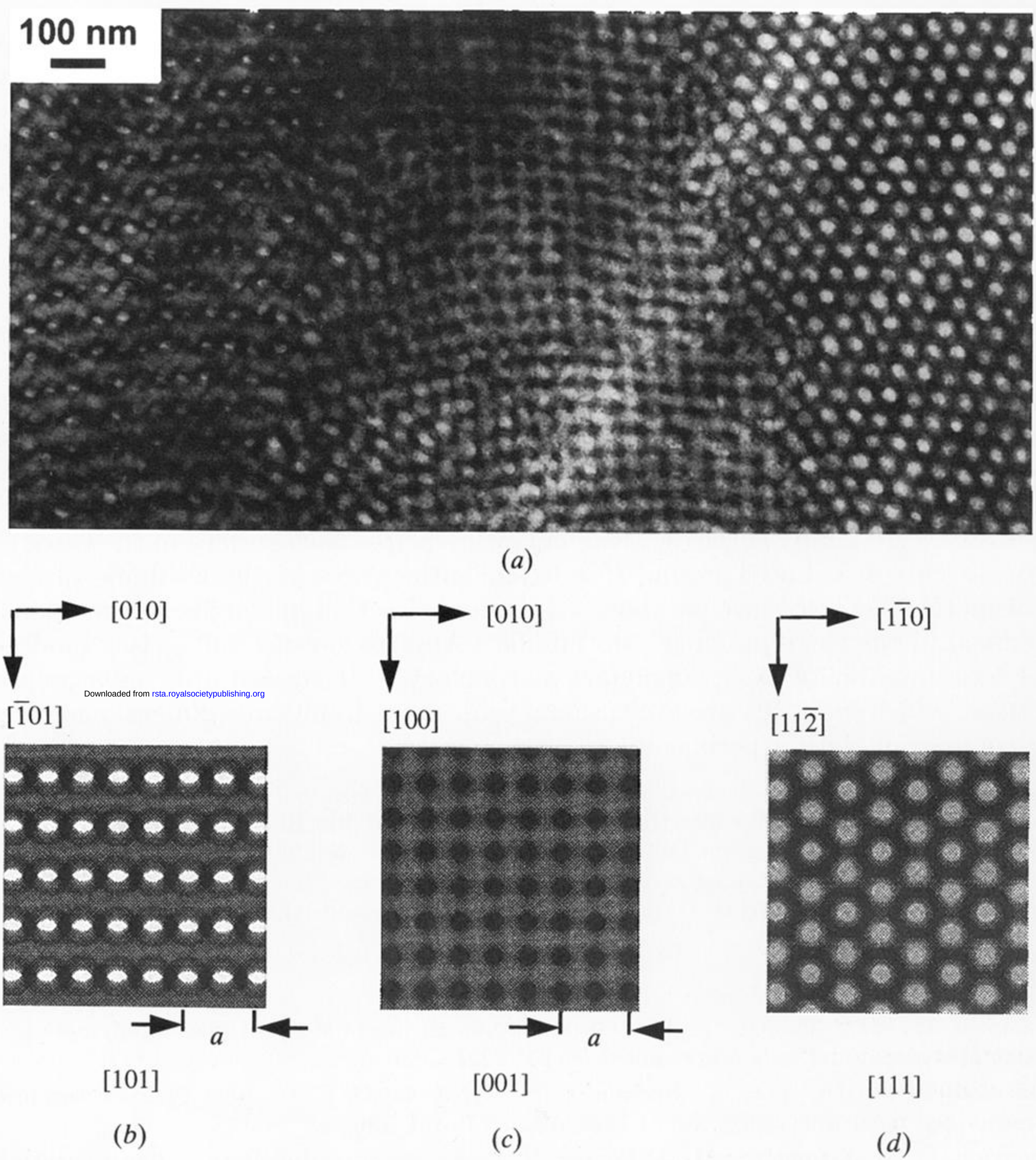

igure 6. (*a*) Transmission electron micrograph of a microphase separated block copolymer. hree different two-dimensionally ordered patterns are apparent, each separated from the oth- s by distinct grain boundaries. The symmetries present in these two-dimensional patterns iggest a tricontinuous morphology with cubic symmetry. Using TEMsim, projections (*b*)–(*d*) ere simulated from nested D (diamond) surfaces with $t = \pm 0.694$, having volume fractions of pproximately 25/50/25. (*b*) The [110] projection, (*c*) the [100] and (*d*) the [111], all of unit cell ickness, which show good agreement with the micrograph. The estimated sample thickness of at shown in (*a*) is in the range of the 77.1 nm cubic unit cell dimension for double diamond.